ACS central science

http://pubs.acs.org/journal/acscii

Research Article

Thiol-Mediated Uptake of a Cysteine-Containing Nanobody for Anticancer Drug Delivery

Felix Goerdeler, Emelie E. Reuber,[‖] Jost Lühle,[‖] Sabrina Leichnitz, Anika Freitag, Ruslan Nedielkov, Raluca Groza, Helge Ewers, Heiko M. Möller, Peter H. Seeberger,* and Oren Moscovitz*

Cite This: *ACS Cent. Sci.* 2023, 9, 1111−1118

Read Online

ACCESS | Metrics & More | Article Recommendations | Supporting Information

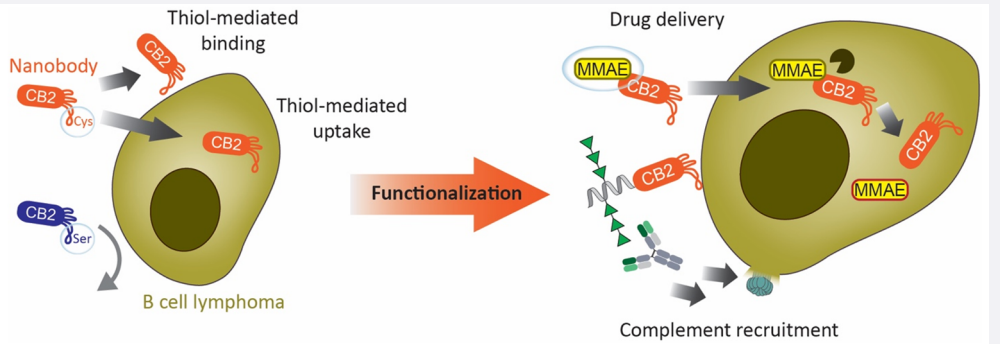

ABSTRACT: The identification of tumor-specific biomarkers is one of the bottlenecks in the development of cancer therapies. Previous work revealed altered surface levels of reduced/oxidized cysteines in many cancers due to overexpression of redox-controlling proteins such as protein disulfide isomerases on the cell surface. Alterations in surface thiols can promote cell adhesion and metastasis, making thiols attractive targets for treatment. Few tools are available to study surface thiols on cancer cells and exploit them for theranostics. Here, we describe a nanobody (CB2) that specifically recognizes B cell lymphoma and breast cancer in a thiol-dependent manner. CB2 binding strictly requires the presence of a nonconserved cysteine in the antigen-binding region and correlates with elevated surface levels of free thiols on B cell lymphoma compared to healthy lymphocytes. Nanobody CB2 can induce complement-dependent cytotoxicity against lymphoma cells when functionalized with synthetic rhamnose trimers. Lymphoma cells internalize CB2 via thiol-mediated endocytosis which can be exploited to deliver cytotoxic agents. CB2 internalization combined with functionalization forms the basis for a wide range of diagnostic and therapeutic applications, rendering thiol-reactive nanobodies promising tools for targeting cancer.

INTRODUCTION

Non-Hodgkin B cell lymphoma is one of the most common cancer types, affecting about 2% of men and women during their lifetime.[1] The main treatment strategy combines the antibody rituximab with chemotherapy, which in general also affects healthy cells.[2] Therefore, less harmful treatment options are highly desirable. The key challenge for developing safe and efficient cancer treatments is the identification of cancer-specific targets. In this respect, the extracellular cancer microenvironment has been an ample source for new biomarkers.[3] Previous work unveiled that the extracellular redox state of many cancers is significantly altered compared to healthy tissues.[4−6] Redox-controlling proteins, such as protein disulfide isomerases (PDIs) or the thioredoxin system, show high expression levels in various tumors.[4,7,8] Notably, the inhibition of PDIs reduces cancer proliferation, rendering PDIs promising therapeutic targets.[7−9] Thioredoxin and PDIs catalyze thiol−disulfide exchange reactions, leading to altered levels of reduced or oxidized protein disulfide bridges. For instance, recent evidence confirms that free thiol groups on the surface of breast cancer cells promote cell adhesion and metastasis.[5] The presence of reduced surface cysteines on cancer cells was also exploited as a vantage point for small thiol-functionalized compounds or peptides that bind to surface thiols resulting in cellular uptake.[10−12]

Nanobodies (Nbs) are the smallest antigen-binding fragments from heavy-chain-only antibodies, exclusively found in camelids (VHH) and cartilaginous fish (VNAR). Their single-domain nature allows straightforward expression in bacterial systems. Compared to conventional IgG antibodies (Abs) of approximately 150 kDa, their small size (approximately 15

Received: February 9, 2023
Published: May 11, 2023

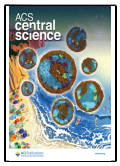

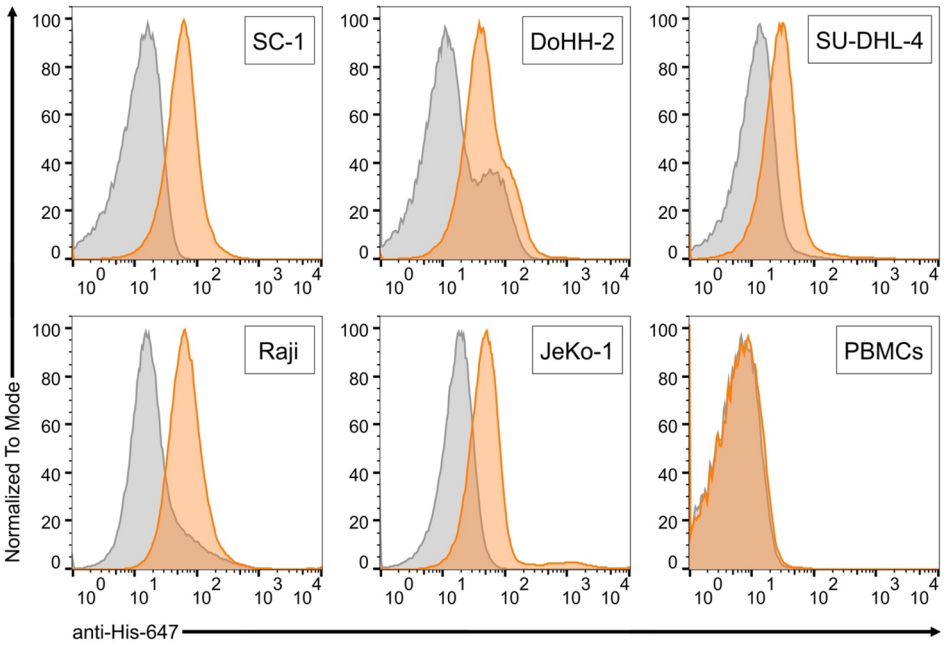

Figure 1. CB2 specifically binds several subtypes of B cell lymphoma. Flow cytometry binding assays with different lymphoma cell lines and healthy human PBMCs. Orange histograms show CB2 binding, gray histograms is secondary antibody control. Screened cells are SC-1 (follicular lymphoma), DoHH-2 (follicular lymphoma), SU-DHL-4 (diffuse large B cell lymphoma), Raji (Burkitt's lymphoma), JeKo-1 (mantle cell lymphoma), and healthy human PBMCs. CB2 (24 μM) binding after 60 min was detected with anti-His-647 Ab (Rockland Inc., 1:500) targeting CB2's C-terminal His-tag.

kDa) enables Nbs to reach less accessible antigens while maintaining high affinity and stability. Functionalization conveys additional desired properties to Nbs, such as fluorescence, cytotoxicity, or cell internalization.[13] Introducing positive charges, either directly into the Nb framework or by fusing a charged peptide, leads to rapid cellular uptake of the engineered Nbs.[14,15]

In human blood, endogenous Abs against a variety of small molecules and glycans are highly abundant because these molecules are recognized as nonself by the immune system.[16,17] For example, rhamnose (Rha) is found in many bacterial polysaccharides, and humans produce anti-Rha Abs due to constant exposure to bacteria in their environment. To exploit these naturally occurring anti-Rha Abs for cancer therapy, cancer cells have been labeled with rhamnose using rhamnose-functionalized liposomes or antibodies.[18,19] Once cancer cells are rhamnose-tagged, anti-Rha Abs from human serum recognize the cells and activate downstream immune pathways, such as the complement cascade, leading to cancer cell death in vitro and in vivo.[18,19]

Here we describe CB2, a Nb discovered by serendipity that specifically binds to lymphoma and breast cancer via a novel thiol-dependent binding mode, followed by internalization of the Nb. We show that CB2 binding and internalization correlate with higher surface levels of reduced cysteines on lymphoma cells compared to healthy lymphocytes and that CB2 can be easily functionalized for different applications.

RESULTS AND DISCUSSION

CB2 Recognizes Several B Cell Lymphoma Cell Lines but Not Healthy Lymphocytes. As part of a previous study for Nb generation,[20] we screened several Nb candidates for binding to antigens that we had used to immunize an alpaca. In parallel, binding to several B cell lymphoma cell lines was tested by flow cytometry. By serendipity, we found one Nb candidate, named CB2, with surprising binding activity: While CB2 did not recognize any of the antigens used for immunization, it reliably bound to the B cell lymphoma cell lines SC-1, Raji, Jeko-1, DOHH-2, and SU-DHL-4, representing several subtypes of B cell lymphoma (Figure 1). In contrast, healthy human peripheral blood mononuclear cells (PBMCs) were not recognized by CB2 (Figure 1).

To assess the applicability of CB2 against other cancer types, we also screened CB2 binding to T cell leukemia, using Jurkat cells, and to breast cancer, using nonmetastatic MCF-7 and highly metastatic, triple-negative MDAMB-231 cell lines. Interestingly, CB2 recognized both breast cancer models with high specificity but did not bind to nontumorigenic breast cells of the MCF-10A cell line or to Jurkat cells (Figure S1C,D). Since we observed the strongest binding with follicular lymphoma cell line SC-1, we chose these cells for further characterization of CB2 binding. First, we determined the level of CB2 binding to SC-1 cells over time by flow cytometry and found no differences between incubation for 30 min, 1 h, or 2 h (Figure S1B). On-cell affinity measurements revealed an apparent dissociation constant of CB2 in the low micromolar range (K_D* = 6.3 ± 0.4 μM) (Figure S1A). Based on these findings, we were intrigued to determine the molecular basis of CB2's specificity for lymphoma cells.

Lymphoma Cells Display Higher Levels of Accessible Surface Thiol Groups than Healthy Lymphocytes. During CB2 purification, a substantial part of the protein was obtained as dimers, which are not formed in the presence of reducing agents such as beta-mercaptoethanol or dithiothreitol (DTT) (Figure S2A,B). We identified a cysteine residue in the complementarity-determining region 3 (CDR3) of CB2 at position 105 and speculated that CB2 interaction with cancer cells may be based on thiol−thiol interactions.

https://doi.org/10.1021/acscentsci.3c00177
ACS Cent. Sci. 2023, 9, 1111−1118

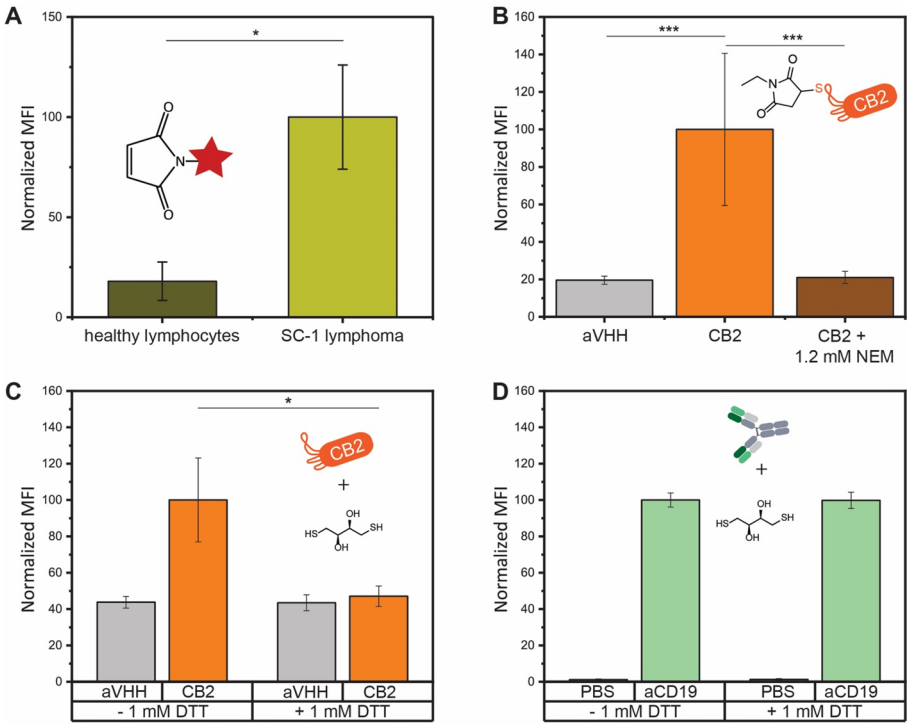

Figure 2. Altered surface thiol levels on lymphoma cells mediate CB2 binding. (A) Flow cytometry quantification of reduced surface thiols on lymphoma cells and healthy lymphocytes. (B) CB2 binding to SC-1 cells is completely lost after preincubation of CB2 with *N*-ethylmaleimide. (C, D) Binding to SC-1 cells in the presence or absence of 1 mM DTT. (C) CB2 binding is abolished in the presence of DTT. For panels B–D, cells were incubated with 24 μM nanobody for 60 min. (D) The binding of the anti-CD19 Ab (positive control) is not affected by DTT. Values represent mean fluorescence intensity (MFI) from three independent experiments. Error bars represent the standard error of the mean (SEM). Differences were tested for significance using one-way ANOVA followed by Tukey's post hoc test with (*) $p < 0.05$, (**) $p < 0.01$, (***) $p < 0.001$.

Previous work revealed that the intra- and extracellular redox state of cancer cells is often altered in the course of cancer progression, for instance, due to PDI overexpression.[4,5,7,8] However, we could not find any quantitative data on the amounts of free thiol groups on lymphoma cells. Therefore, we set out to compare the level of free thiols on SC-1 cells and healthy lymphocytes using the thiol probe Alexa647-maleimide. After verifying by confocal microscopy that this probe is not internalized by cells and remains on the cell surface (Figure S4), we quantified the surface thiol levels of cells by flow cytometry. Indeed, SC-1 lymphoma cells showed approximately 5-fold increased fluorescence compared to healthy lymphocytes, suggesting higher levels of accessible surface thiol groups on lymphoma cells (Figure 2A).

CB2 Binding Requires a Reduced, Accessible Thiol Group. To determine whether CB2 binding is mediated by thiol–thiol interactions, we performed a variety of inhibition experiments (Figure 2B–D, Figure S3). When repeating CB2 binding assays in the presence of the reducing agent DTT, CB2 binding to SC-1 cells was completely abolished (Figure 2C). The same loss of binding was observed in the presence of TCEP or glutathione (Figure S3). The binding of anti-CD19 Ab, used as a positive control, remained unchanged in the presence of DTT, demonstrating that mildly reducing conditions do not interfere with Ab binding in general (Figure 2D).

In addition, we also preincubated CB2 with the thiol quenching agent *N*-ethylmaleimide (NEM) before probing cell binding and found that NEM-treated CB2 lost binding to SC-1 cells, further highlighting the crucial role of a free thiol group for CB2 binding (Figure 2B).

Cysteine 105 Is Essential for CB2 Binding. Encouraged by our results, we generated a C105S mutant of CB2 (hereon ^{C105S}CB2) to examine the role of this specific residue in cell recognition (Figure S2A). Indeed, ^{C105S}CB2 failed to bind SC-1 cells when testing its activity in flow cytometry assays (Figure 3A,B). To exclude the possibility that the mutation disrupts the structure of CB2, we acquired ^{1}H–^{15}N HSQC NMR spectra of ^{15}N-labeled CB2 and ^{C105S}CB2. The spectra showed only minimal shifts in the signals (Figure S2C), indicating that the mutant retained the same folding as CB2. To further corroborate the flow cytometry data, we also incubated SC-1 cells with CB2 or ^{C105S}CB2 and stained bound Nb with anti-6×His-Alexa647 Ab for confocal microscopy (Figure 3C,D). Indeed, CB2 binding was completely abolished for the C105S mutant, confirming our previous observation. Cysteine 105 hence plays an essential role in the recognition of SC-1 cells by CB2.

Rhamnose-Functionalized CB2 Triggers Complement Activation against Lymphoma Cells. Due to the established role of rhamnose as an antibody-recruiting molecule (ARM), we reasoned that functionalization with rhamnose could enable CB2 to recruit Abs to lymphoma cells (Figure 4A). In this model, Ab recruitment would trigger a downstream immune response by activating the complement cascade, ultimately leading to cancer cell death.

When screening Abs isolated from healthy human serum on a synthetic glycan array for the presence of anti-Rha Abs, we could detect both IgG and IgM Abs binding to rhamnose

https://doi.org/10.1021/acscentsci.3c00177
ACS Cent. Sci. 2023, 9, 1111–1118

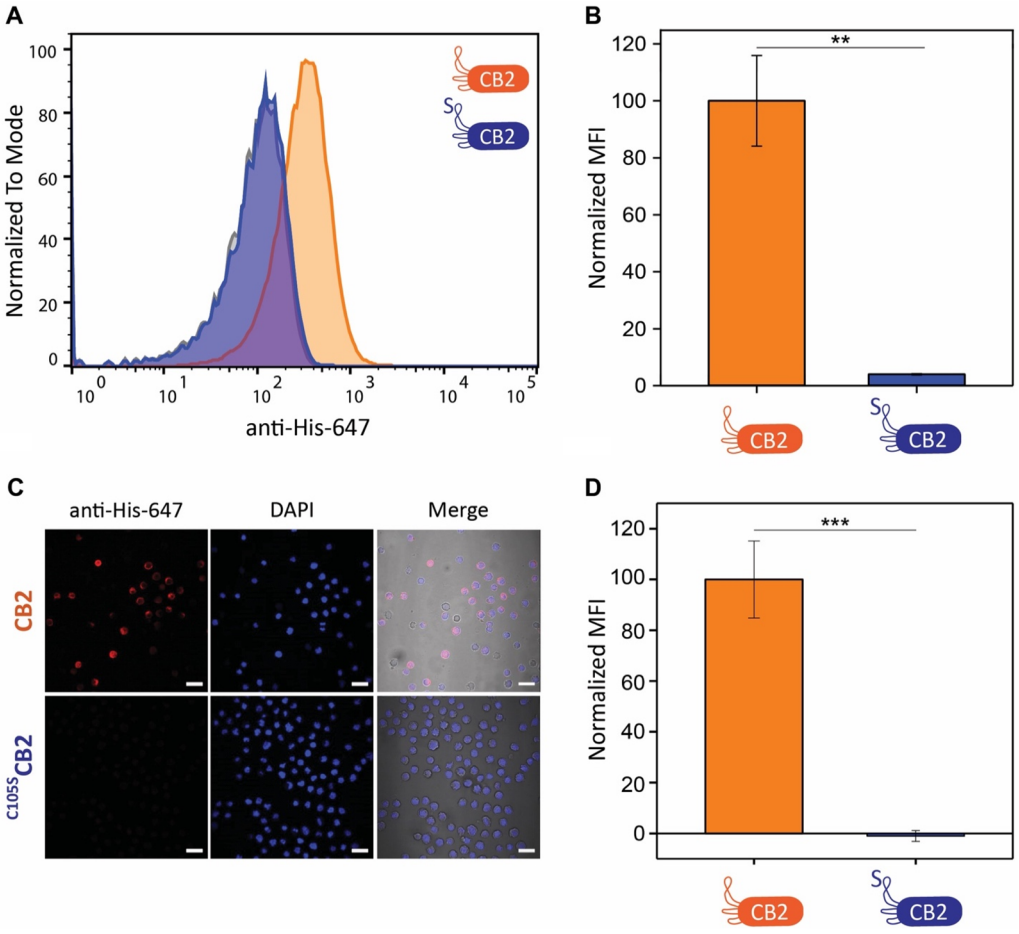

Figure 3. ^{C105S}CB2 is unable to bind B cell lymphoma. (A) Representative flow cytometry histograms of a binding assay to SC-1 cells. Secondary antibody control is displayed in gray. (B) Quantification of flow cytometry binding assays of CB2 and ^{C105S}CB2 to SC-1 cells (N = 3). Normalized MFI is significantly reduced for ^{C105S}CB2. (C) Confocal fluorescence microscopy images of SC-1 cells incubated with CB2 and ^{C105S}CB2, respectively. Scale bars correspond to 20 μm. Red, anti-His-647; blue, DAPI; grayscale, transmission light. (D) Quantification of fluorescence microscopy images shown in panel A (N = 2 and n > 170 cells). Normalized MFI is significantly reduced in the case of ^{C105S}CB2. Cells were incubated with 24 μM CB2 or ^{C105S}CB2 for 60 min, followed by incubation with detection Ab anti-His-647 (1:500) for 60 min. Values represent mean ± SEM. Differences were tested for significance using one-way ANOVA followed by Tukey's post hoc test with (*) $p < 0.05$, (**) $p < 0.01$, (***) $p < 0.001$.

(Figure 4C). We then coupled glycylated rhamnose monosaccharides to the C-terminus of CB2 using sortase A (srtA) to test Ab recruitment to cells. However, we could not detect any complement-dependent cytotoxicity (CDC) of CB2-Rha on SC-1 cells (data not shown). Previous work on ARMs suggested that attaching a single ARM moiety might not be sufficient to recruit Abs, as anti-Rha Abs in human serum are formed due to natural exposure to Rha-decorated pathogens, and bacterial capsular polysaccharides often contain several Rha moieties in a row.[19,21] Since rha(α1−2)rha(α1−2)rha (hereon Rha_3) forms part of the surface glycans of both *Klebsiella* and *Streptococcus*,[22,23] we compared serum IgG/IgM levels against a single Rha or Rha_3 on glycan arrays. As a control, we measured the Ab titer against man(α1−2)man-(α1−2)man (Man_3). As expected, IgM/IgG titers both against Rha and Rha_3 were significantly higher compared to Man_3 (Figure 4C). Interestingly, we could see a significant 3-fold increase in fluorescence for IgGs against Rha_3 compared to Rha, suggesting that more IgGs are present against Rha_3 than against Rha (Figure 4C).

Therefore, we designed the multivalent rhamnose conjugate CB2-Rha-thFF03 (Figure 4B and Figure S6), consisting of CB2 and a C-terminally coupled synthetic glycopeptide, decorated with several Rha_3, and tested its effect on cells. Antihuman IgG Ab was used as a positive control for complement activation as it recognizes the abundant surface IgGs on B cell lymphoma. Indeed, CB2-Rha-thFF03 reliably induced complement activation against SC-1 cells, measured by an increase in dead SC-1 cells after incubation with CB2-Rha-thFF03, human anti-Rha Abs, and active complement (Figure 4D). Compared to the 100% cytotoxic effect of the positive control, CB2-Rha-thFF03 achieved 76% cytotoxicity. In contrast, unconjugated CB2 showed only 36% cytotoxicity, corresponding to unspecific complement activity (Figure 4D). This demonstrates the ability of CB2-Rha-thFF03 to recruit Abs and complement factors to lymphoma cells.

Based on our observations, we recommend employing a multivalent display of rhamnose multimers for antibody recruitment/complement activity assays. First, Rha_3 showed much higher Ab response levels than Rha when investigating pooled human serum on a glycan array. Second, a single Rha_3 attached to the C-terminus of CB2 was insufficient to recruit Abs to SC-1 cells, and we only observed complement-

https://doi.org/10.1021/acscentsci.3c00177
ACS Cent. Sci. 2023, 9, 1111−1118

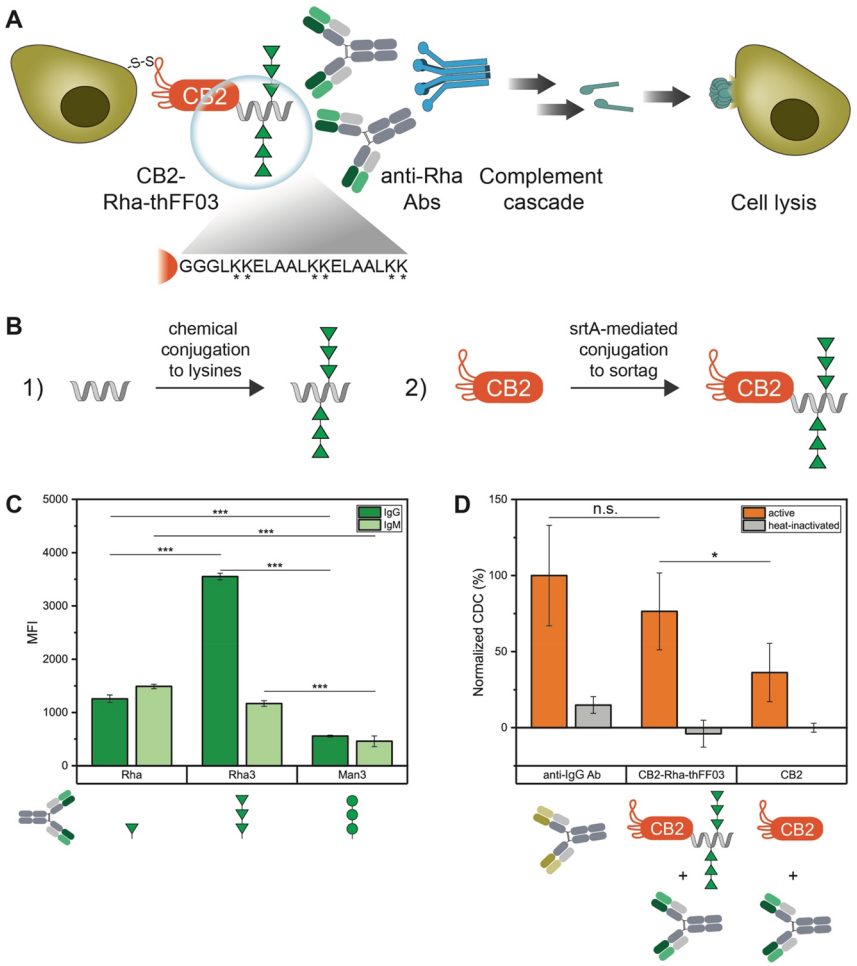

Figure 4. Rhamnose-functionalized CB2 induces CDC against B cell lymphoma. (A) Model for complement activation. CB2-Rha-thFF03 recruits endogenous anti-Rha Abs to lymphoma cells via its Rha moieties. Anti-Rha Abs activate the complement cascade, leading to cell lysis. Magnified: The thFF03 peptide contains six lysines for the chemical conjugation of Rha_3. (B) Illustration of the conjugation approach. First, several Rha_3 moieties are attached to the lysine side chains of the thFF03 peptide (1). Then, the sortase reaction is used to couple rhamnosylated thFF03 to the C-terminus of CB2 (2). (C) Glycan array confirming the presence of anti-Rha Abs in human serum. Note that Rha_3 is recognized by more IgGs isolated from human serum than Rha monomers. (D) Complement-dependent cytotoxicity assay. Note that CB2-Rha-thFF03 shows increased cytotoxicity compared to CB2. Antihuman IgG Ab was included as a positive control. Cells were incubated with mixtures of CB2 or CB2-Rha-thFF03 (0.4 mg/mL = 24 μM) and human Abs (0.2 mg/mL) for 1 h at RT, followed by incubation with rabbit complement for 2 h at 37 °C. Values are normalized to the positive control (100%) and represent mean ± SEM (N = 3), (*) $p < 0.05$, (**) $p < 0.01$, (***) $p < 0.001$.

dependent cytotoxicity with the multivalent construct CB2-Rha-thFF03.

CB2 Binding Causes Cellular Uptake via Clathrin-Mediated Endocytosis. Since previous studies showed improved cellular uptake of thiol-functionalized peptides,[24] we hypothesized that CB2 could also be internalized by SC-1 cells. To test this hypothesis, we generated Cy3-functionalized CB2 and ^{C105S}CB2 via a combination of srtA-mediated conjugation and click chemistry (Figure 5A and Figure S7A,B). After verifying that CB2−Cy3 conjugates still retain binding activity (Figure S7C,D), we examined potential cellular uptake using confocal microscopy. Indeed, CB2−Cy3 is readily internalized by SC-1 cells as fluorescence accumulates inside the cells with CB2−Cy3 but not with ^{C105S}CB2−Cy3, demonstrating the thiol-dependent nature of the binding mechanism which is a prerequisite for internalization (Figure S8). Interestingly, internalization is significantly reduced in the presence of clathrin-mediated endocytosis inhibitors dynasore or chlorpromazine (Figure S8), supporting the notion that CB2−Cy3 is endocytosed by SC-1 cells. To validate this hypothesis, we next performed colocalization experiments, imaging live SC-1 cells incubated with CB2−Cy3 or ^{C105S}CB2−Cy3 as well as the lysosomal marker lysotracker (Figure 5B−E). Colocalization of CB2−Cy3 with lysotracker was already significantly increased after 30 min, and we detected ∼40% of colocalization after 4 h. In contrast, no significant uptake of ^{C105S}CB2−Cy3 was observed even after 4 h of incubation (Figure 5B−E). These findings nicely corroborate our endocytosis inhibition data and strongly suggest that the primary mode of thiol-mediated CB2 uptake is endocytosis.

CB2 Internalization Can Be Exploited for Drug Delivery. To determine whether CB2 internalization can be used for potential therapeutic application, the srtA reaction was used to couple the antineoplastic agent monomethyl auristatin E (MMAE) to the C-terminus of CB2 (Figure S9A,B). Due to its high potency and resulting off-target toxicity, MMAE cannot be administered alone but only when conjugated to an antibody or nanobody conveying target specificity.[25] The commercially available MMAE construct for sortase-mediated

https://doi.org/10.1021/acscentsci.3c00177
ACS Cent. Sci. 2023, 9, 1111−1118

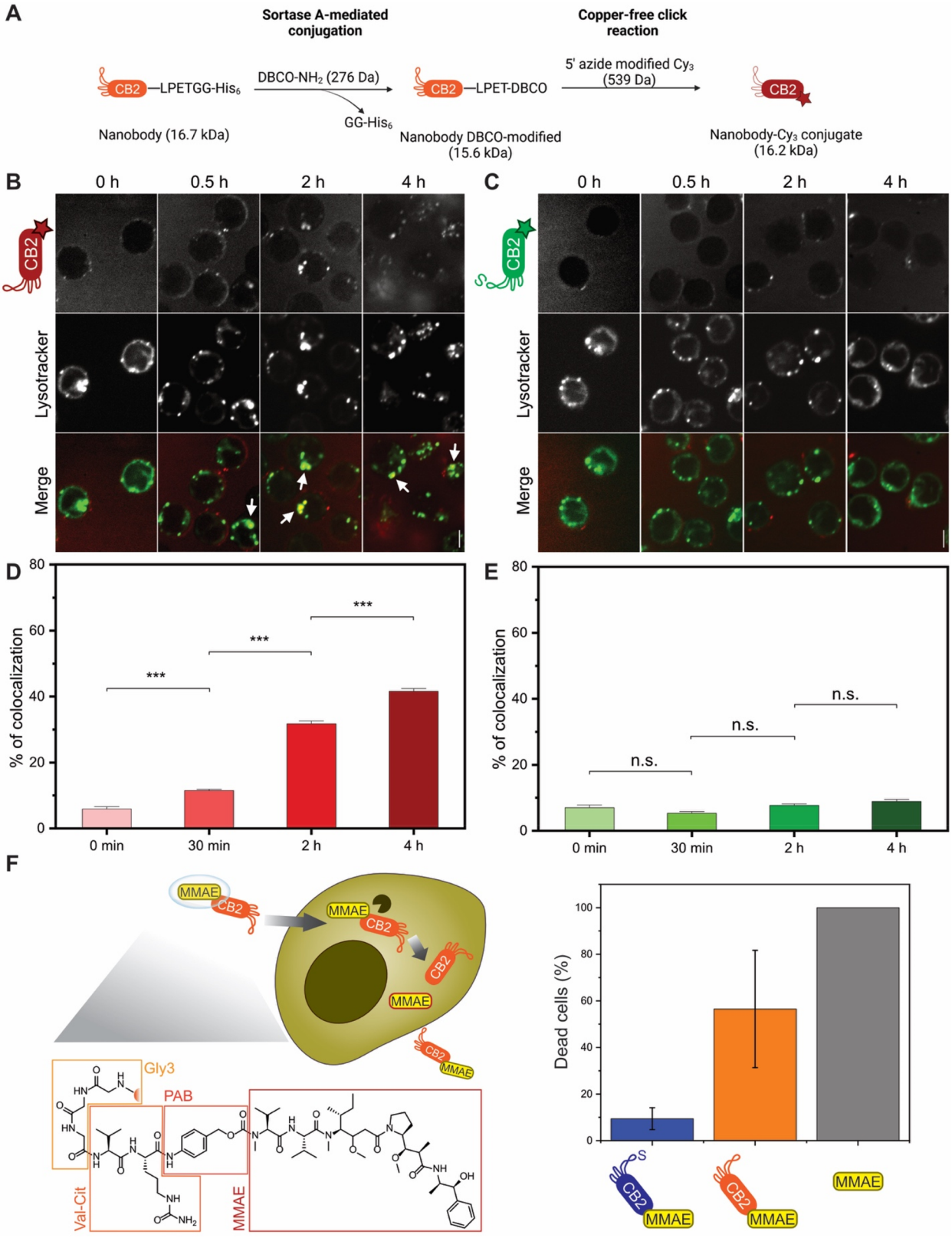

Figure 5. CB2 can be internalized by B cell lymphoma and used for drug delivery. (A) Illustration of the conjugation approach. The C-terminus of CB2 is functionalized with a dibenzocyclooctyne (DBCO) group using the sortase reaction. Subsequently, Cy3-azide is attached to CB2-DBCO via copper-free click chemistry, yielding fluorescent CB2 linked to Cy3 via a triazole moiety. (B–E) Nanobody internalization assay. Confocal fluorescence microscopy images of live SC-1 cells incubated with 100 μg of (B) CB2–Cy3 or (C) ^{C105S}CB2–Cy3 for increasing time intervals (0 min, 30 min, 2 h, 4 h). Top, nanobody; bottom, lysotracker. Colors in merge: red = Cy3, green = lysotracker. White arrows indicate colocalization between nanobody and lysotracker. Scale bar = 5 μm. Quantification of colocalization in live-cell microscopy of lysotracker with (D) CB2–Cy3 or (E) ^{C105S}CB2–Cy3. Values represent mean ± SEM (n > 300 cells/time point from three independent experiments), (***) p < 0.001, (n.s.) p > 0.05. Note that colocalization with lysotracker significantly increases over time for CB2–Cy3, whereas ^{C105S}CB2–Cy3 does not accumulate in the

https://doi.org/10.1021/acscentsci.3c00177
ACS Cent. Sci. 2023, 9, 1111–1118

Figure 5. continued

lysosomes. (F) Drug delivery with internalizing CB2. Left panel: Proposed mechanism of action. MMAE is coupled to CB2 via a cleavable linker using srtA. Val−cit = valine−citrulline, PAB = para-aminobenzylcarbamate, MMAE = monomethyl auristatin E. MMAE is released inside the cell by cathepsin (black) cleaving between val−cit. Right panel: Cytotoxicity assay with SC-1 cells. Dead cells (%) after 48 h incubation with 10 nM CB2-MMAE, ^{C105S}CB2-MMAE, or MMAE. Note that only CB2-MMAE and MMAE alone show considerable cytotoxic activity. Cytotoxicity was measured using the CCK8 kit and normalized to 100% and 0% based on positive (TritonX) and negative (unconjugated CB2) controls, respectively. Values represent mean ± SEM (N = 3).

conjugation consists of the active compound and a valine−citrulline linker that is cleaved by intracellular cathepsins, thereby releasing the drug inside the cell (Figure 5F).

After confirming that CB2-MMAE retains binding activity (Figure S9C), we incubated lymphoma cells with 10 nM MMAE, CB2-MMAE, ^{C105S}CB2-MMAE, or nonconjugated CB2 and measured cell viability after 48 h (Figure 5F). Cells treated with 1% Triton X-100 or unconjugated CB2 served as positive (100% dead cells) and negative (0% dead cells) controls, respectively. After 48 h, CB2-MMAE had killed ∼60% of cells compared to 100% dead cells observed with unconjugated MMAE. In contrast, ^{C105S}CB2-MMAE killed only ∼10% of cells (Figure 5F). These results demonstrate that CB2 can indeed be used to deliver cytotoxic agents inside lymphoma cells, rendering CB2-MMAE conjugates a promising tool to circumvent MMAE's high off-target toxicity.

Interestingly, CB2 internalization is observed even though we could not detect changes in the level of surface-bound CB2 within the time scale of CB2 internalization (Figure 5B−E, Figure S1). Compared to surface-bound CB2, the amount of internalized CB2 might be too little to be detected by our approach. However, the fact that CB2 binding and internalization are observed within a similar time scale suggests that CB2 targets distinct populations of membrane proteins. In this model, some protein targets remain on the surface while others become endocytosed upon CB2 binding, allowing for extra- and intracellular targeting of lymphoma cells with CB2. Indeed, Rha_3-functionalized CB2 reliably recruited anti-Rha Abs to the surface of SC-1 cells, thereby inducing complement-dependent cytotoxicity. At the same time, MMAE-functionalized CB2 was able to deliver MMAE to the cytosol of SC-1 cells, causing drug-induced cytotoxicity.

CONCLUSIONS

With CB2, we describe the first nanobody that recognizes and internalizes into lymphoma cells in a thiol-dependent manner. We demonstrate that CB2's interaction with B cell lymphoma requires the presence of a free thiol group at cysteine 105. While the precise CB2 epitopes on lymphoma cells remain to be elucidated, CB2 binding correlates with increased surface levels of accessible reduced thiol groups on B cell lymphoma compared to healthy lymphocytes, suggesting specificity based on altered redox reactivity. The thiol-dependent nature of CB2 binding also leads to CB2 uptake by B cell lymphoma. We show that CB2 internalization opens up a vast array of potential applications for cancer diagnostics and therapeutics. In addition to drug delivery, a diagnostic use of CB2 seems promising as fluorescently labeled CB2 could be directly used for tumor imaging in vivo. Bispecific constructs are also conceivable, combining CB2 with a Nb against other lymphoma biomarkers such as CD19. This could potentially decrease off-target binding and, at the same time, lead to tumor inhibition via receptor internalization. Alternatively, CB2 could be employed to develop chimeric antigen receptor (CAR) T cells, rendering it applicable for immunotherapy of B cell lymphoma. Finally, CB2 also specifically recognized breast cancer, including triple-negative MDAMB-231 cells. These data expand the potential list of targets for thiol-based therapeutics, providing exciting opportunities for CB2 application against additional cancer types.

ASSOCIATED CONTENT

Supporting Information

The Supporting Information is available free of charge at https://pubs.acs.org/doi/10.1021/acscentsci.3c00177.

Detailed materials and methods; additional CB2 binding assays (time course, different concentrations for apparent affinity, in the presence of further reducing agents, with additional cancer and control cell lines); biochemical characterization of CB2 (dimerization/reduction assays, NMR); cell surface staining with Alexa647-maleimide; NMR spectra of Rha_3; CB2 conjugation to Rha_3/Cy3/MMAE; and endocytosis inhibition assay (PDF)

AUTHOR INFORMATION

Corresponding Authors

Peter H. Seeberger − *Department of Biomolecular Systems, Max Planck Institute of Colloids and Interfaces, 14476 Potsdam, Germany; Institute of Chemistry and Biochemistry, Freie Universität Berlin, 14195 Berlin, Germany*; Email: peter.seeberger@mpikg.mpg.de

Oren Moscovitz − *Department of Biomolecular Systems, Max Planck Institute of Colloids and Interfaces, 14476 Potsdam, Germany*; orcid.org/0000-0002-6310-2579; Email: oren.moscovitz@mpikg.mpg.de

Authors

Felix Goerdeler − *Department of Biomolecular Systems, Max Planck Institute of Colloids and Interfaces, 14476 Potsdam, Germany; Institute of Chemistry and Biochemistry, Freie Universität Berlin, 14195 Berlin, Germany*

Emelie E. Reuber − *Department of Biomolecular Systems, Max Planck Institute of Colloids and Interfaces, 14476 Potsdam, Germany; Institute of Chemistry and Biochemistry, Freie Universität Berlin, 14195 Berlin, Germany*

Jost Lühle − *Department of Biomolecular Systems, Max Planck Institute of Colloids and Interfaces, 14476 Potsdam, Germany; Institute of Chemistry and Biochemistry, Freie Universität Berlin, 14195 Berlin, Germany*

Sabrina Leichnitz − *Department of Biomolecular Systems, Max Planck Institute of Colloids and Interfaces, 14476 Potsdam, Germany; Institute of Chemistry and Biochemistry, Freie Universität Berlin, 14195 Berlin, Germany*

Anika Freitag − *Department of Biomolecular Systems, Max Planck Institute of Colloids and Interfaces, 14476 Potsdam, Germany; Institute of Chemistry, University of Potsdam, 14476 Potsdam, Germany*

https://doi.org/10.1021/acscentsci.3c00177
ACS Cent. Sci. 2023, 9, 1111−1118

Ruslan Nedielkov − *Institute of Chemistry, University of Potsdam, 14476 Potsdam, Germany*
Raluca Groza − *Institute of Chemistry and Biochemistry, Freie Universität Berlin, 14195 Berlin, Germany*
Helge Ewers − *Institute of Chemistry and Biochemistry, Freie Universität Berlin, 14195 Berlin, Germany*
Heiko M. Möller − *Institute of Chemistry, University of Potsdam, 14476 Potsdam, Germany*

Complete contact information is available at: https://pubs.acs.org/10.1021/acscentsci.3c00177

Author Contributions

[‖]E.E.R. and J.L. contributed equally to this work.

Notes

The authors declare no competing financial interest.

■ ACKNOWLEDGMENTS

Generous financial support by the Max Planck Society is gratefully acknowledged. This work was supported by Deutsche Forschungsgemeinschaft (RTG2046 for F.G. and J.L., CRC1449 for S.L., and RTG2327 for R.G. and H.E.). The authors thank Dr. Peter Sondermann for reviewing the manuscript and providing helpful feedback.

■ REFERENCES

(1) *Cancer Stat Facts: Non-Hodgkin Lymphoma*; National Cancer Institute. https://seer.cancer.gov/statfacts/html/nhl.html (accessed 2022-06-26).
(2) Van Der Kolk, L. E.; Grillo-López, A. J.; Baars, J. W.; Hack, C. E.; Van Oers, M. H. J. Complement Activation Plays a Key Role in the Side-Effects of Rituximab Treatment. *Br. J. Hamaetol.* **2001**, *115* (4), 807−811.
(3) Brassart-Pasco, S.; Brézillon, S.; Brassart, B.; Ramont, L.; Oudart, J. B.; Monboisse, J. C. Tumor Microenvironment: Extracellular Matrix Alterations Influence Tumor Progression. *Frontiers in Oncology.* **2020**, *10*, 397.
(4) Arnér, E. S. J.; Holmgren, A. The Thioredoxin System in Cancer. *Semin. Cancer Biol.* **2006**, *16* (6), 420−426.
(5) Popielarski, M.; Ponamarczuk, H.; Stasiak, M.; Watała, C.; Świątkowska, M. Modifications of Disulfide Bonds in Breast Cancer Cell Migration and Invasiveness. *Am. J. Cancer Res.* **2019**, *9* (8), 1554−1582.
(6) Sahaf, B.; Heydari, K.; Herzenberg, L. A.; Herzenberg, L. A. Lymphocyte Surface Thiol Levels. *Proc. Natl. Acad. Sci. U. S. A.* **2003**, *100* (7), 4001.
(7) Robinson, R. M.; Reyes, L.; Duncan, R. M.; Bian, H.; Reitz, A. B.; Manevich, Y.; McClure, J. J.; Champion, M. M.; Chou, C. J.; Sharik, M. E.; Chesi, M.; Bergsagel, P. L.; Dolloff, N. G. Inhibitors of the Protein Disulfide Isomerase Family for the Treatment of Multiple Myeloma. *Leukemia* **2019**, *33* (4), 1011−1022.
(8) Kuo, T. F.; Chen, T. Y.; Jiang, S. T.; Chen, K. W.; Chiang, Y. M.; Hsu, Y. J.; Liu, Y. J.; Chen, H. M.; Yokoyama, K. K.; Tsai, K. C.; Yeh, H. H.; Chen, Y. R.; Yang, M. T.; Yang, C. Y.; Yang, W. C. Protein Disulfide Isomerase A4 Acts as a Novel Regulator of Cancer Growth through the Procaspase Pathway. *Oncogene* **2017**, *36* (39), 5484−5496.
(9) Tufo, G.; Jones, A. W. E.; Wang, Z.; Hamelin, J.; Tajeddine, N.; Esposti, D. D.; Martel, C.; Boursier, C.; Gallerne, C.; Migdal, C.; Lemaire, C.; Szabadkai, G.; Lemoine, A.; Kroemer, G.; Brenner, C. The Protein Disulfide Isomerases PDIA4 and PDIA6Mediate Resistance to Cisplatin-Induced Cell Death in Lung Adenocarcinoma. *Cell Death Differ.* **2014**, *21* (5), 685−695.
(10) Aubry, S.; Burlina, F.; Dupont, E.; Delaroche, D.; Joliot, A.; Lavielle, S.; Chassaing, G.; Sagan, S. Cell-surface Thiols Affect Cell Entry of Disulfide-conjugated Peptides. *FASEB J.* **2009**, *23* (9), 2956−2967.
(11) Gasparini, G.; Sargsyan, G.; Bang, E. K.; Sakai, N.; Matile, S. Ring Tension Applied to Thiol-Mediated Cellular Uptake. *Angew. Chemie - Int. Ed.* **2015**, *54* (25), 7328−7331.
(12) Li, T.; Takeoka, S. Enhanced Cellular Uptake of Maleimide-Modified Liposomes via Thiol-Mediated Transport. *Int. J. Nanomedicine* **2014**, *9* (1), 2849−2861.
(13) Schumacher, D.; Helma, J.; Schneider, A. F. L.; Leonhardt, H.; Hackenberger, C. P. R. Nanobodies: Chemical Functionalization Strategies and Intracellular Applications. *Angew. Chemie Int. Ed.* **2018**, *57* (9), 2314−2333.
(14) Bruce, V. J.; Lopez-Islas, M.; McNaughton, B. R. Resurfaced Cell-Penetrating Nanobodies: A Potentially General Scaffold for Intracellularly Targeted Protein Discovery. *Protein Sci.* **2016**, *25* (6), 1129−1137.
(15) Herce, H. D.; Schumacher, D.; Schneider, A. F. L.; Ludwig, A. K.; Mann, F. A.; Fillies, M.; Kasper, M. A.; Reinke, S.; Krause, E.; Leonhardt, H.; Cardoso, M. C.; Hackenberger, C. P. R. Cell-Permeable Nanobodies for Targeted Immunolabelling and Antigen Manipulation in Living Cells. *Nat. Chem.* **2017**, *9* (8), 762−771.
(16) Jakobsche, C. E.; Parker, C. G.; Tao, R. N.; Kolesnikova, M. D.; Douglass, E. F.; Spiegel, D. A. Exploring Binding and Effector Functions of Natural Human Antibodies Using Synthetic Immunomodulators. *ACS Chem. Biol.* **2013**, *8* (11), 2404−2411.
(17) Sheridan, R. T. C.; Hudon, J.; Hank, J. A.; Sondel, P. M.; Kiessling, L. L. Rhamnose Glycoconjugates for the Recruitment of Endogenous Anti-Carbohydrate Antibodies to Tumor Cells. *ChemBioChem.* **2014**, *15* (10), 1393−1398.
(18) Ou, C.; Prabhu, S. K.; Zhang, X.; Zong, G.; Yang, Q.; Wang, L.-X. Synthetic Antibody-rhamnose Cluster Conjugates Show Potent Complement-dependent Cell Killing by Recruiting Natural Antibodies.Pdf. *Chem. - A Eur. J.* **2022**, *28* (16), No. e202200146.
(19) Li, X.; Rao, X.; Cai, L.; Liu, X.; Wang, H.; Wu, W.; Zhu, C.; Chen, M.; Wang, P. G.; Yi, W. Targeting Tumor Cells by Natural Anti-Carbohydrate Antibodies Using Rhamnose-Functionalized Liposomes. *ACS Chem. Biol.* **2016**, *11* (5), 1205−1209.
(20) Khilji, S. K.; Goerdeler, F.; Frensemeier, K.; Warschkau, D.; Lühle, J.; Fandi, Z.; Schirmeister, F.; Chen, Z. A.; Turak, O.; Mallagaray, A.; Boerno, S.; Timmermann, B.; Rappsilber, J.; Seeberger, P. H.; Moscovitz, O. Generation of Glycan-Specific Nanobodies. *Cell Chem. Biol.* **2022**, *29*, 1353.
(21) Sianturi, J.; Manabe, Y.; Li, H. S.; Chiu, L. T.; Chang, T. C.; Tokunaga, K.; Kabayama, K.; Tanemura, M.; Takamatsu, S.; Miyoshi, E.; Hung, S. C.; Fukase, K. Development of α-Gal-Antibody Conjugates to Increase Immune Response by Recruiting Natural Antibodies. *Angewandte Chemie - International Edition* **2019**, *58*, 4526−4530.
(22) Michon, F.; Katzenellenbogen, E.; Kasper, D. L.; Jennings, H. J. Structure of the Complex Group-Specific Polysaccharide of Group B Streptococcus. *Biochemistry* **1987**, *26* (2), 476−486.
(23) Kubler-Kielb, J.; Vinogradov, E.; Ng, W. I.; MacZynska, B.; Junka, A.; Bartoszewicz, M.; Zelazny, A.; Bennett, J.; Schneerson, R. The Capsular Polysaccharide and Lipopolysaccharide Structures of Two Carbapenem Resistant Klebsiella Pneumoniae Outbreak Isolates. *Carbohydr. Res.* **2013**, *369*, 6−9.
(24) Laurent, Q.; Martinent, R.; Lim, B.; Pham, A.-T.; Kato, T.; López-Andarias, J.; Sakai, N.; Matile, S. Thiol-Mediated Uptake. *JACS Au* **2021**, *1* (6), 710−728.
(25) Beck, A.; Goetsch, L.; Dumontet, C.; Corvaïa, N. Strategies and Challenges for the next Generation of Antibody-Drug Conjugates. *Nature Reviews Drug Discovery.* **2017**, *16*, 315.